

# Phase Stability, Oxygen Nonstoichiometry, and Superconductivity Properties of $\text{Bi}_2\text{Sr}_2\text{CaCu}_2\text{O}_{8+\delta}$ and $\text{Bi}_{1.8}\text{Pb}_{0.4}\text{Sr}_2\text{Ca}_2\text{Cu}_3\text{O}_{10+\delta}$

Alexander P. Mozhaev, Serge V. Chernyaev, Yulia V. Badun, and Maxim S. Kuznetsov

Department of Chemistry, Moscow State University, Moscow 119899, Russia

Received November 12, 1993; in revised form April 28, 1994; accepted May 2, 1994

Phase stability of  $\text{Bi}_2\text{Sr}_2\text{CaCu}_2\text{O}_{8+\delta}$  (2212) and  $\text{Bi}_{1.8}\text{Pb}_{0.4}\text{Sr}_2\text{Ca}_2\text{Cu}_3\text{O}_{10+\delta}$  (2223) was studied by means of thermogravimetry, dilatometry, high-temperature resistivity, and the powder X-ray methods in the temperature range 700–1000° and at  $P_{\text{O}_2} = 1-10^{-4.3}$  atm. The existence of a high-temperature (peritectic melting) boundary of phase stability was found. The temperatures of low-temperature phase decomposition were determined in air and under an oxygen atmosphere. The change in oxygen content was determined for the 2212 phase in the temperature range 700–860°C and at  $P_{\text{O}_2} = 0.21-10^{-3.7}$  atm by iodometric analysis of quenched samples. It was found that in the single-phase region, the change in oxygen nonstoichiometry had an insignificant influence on  $T_c$ . It was also shown that the slow cooling of samples led to a significant decrease in  $T_c$  and transport  $j_c$  due to partial phase decomposition. © 1995 Academic Press, Inc.

## 1. INTRODUCTION

Annealing in oxygen of air atmosphere is an inevitable stage in the synthesis of ceramic high-temperature superconductors (HTSC), but the phase transformations which occur during the oxidation and their kinetics are not sufficiently understood. The  $P$ – $T$ – $x$  phase diagram (1) and diffusion coefficients for Bi-HTSC materials have not been studied thoroughly and the information about annealing conditions is empirical (2–6). The influence of oxygen nonstoichiometry and ratio of cation concentrations on superconductivity properties requires a detailed investigation (7–9).

In this paper we present the results of an investigation of the phase stability of  $\text{Bi}_2\text{Sr}_2\text{CaCu}_2\text{O}_{8+\delta}$  (2212) and  $\text{Bi}_{1.8}\text{Pb}_{0.4}\text{Sr}_2\text{Ca}_2\text{Cu}_3\text{O}_{10+\delta}$  (2223), the oxygen nonstoichiometry of  $\text{Bi}_2\text{Sr}_2\text{CaCu}_2\text{O}_{8+\delta}$ , and the correlation between oxygen nonstoichiometry and superconductivity properties.

## 2. EXPERIMENTAL

The samples of 2212 phase were prepared by a spray-drying method using  $\text{Bi}(\text{CH}_3\text{COO})_3$ ,  $\text{Sr}(\text{NO}_3)_2$ ,  $\text{Ca}(\text{NO}_3)_2$ ,

and  $\text{Cu}(\text{NO}_3)_2$  solutions. The salt powder was heated at 820°C (5 hr, in air). The X-ray diffraction pattern of this powder revealed the presence of only one phase. This phase was identified as low- $T_c$   $\text{Bi}_2\text{Sr}_2\text{CaCu}_2\text{O}_{8+\delta}$ . The single-phase 2223 samples were prepared by solid state reaction. The mixture of  $\text{Bi}_2\text{O}_3$ ,  $\text{Pb}_3\text{O}_4$ ,  $\text{Sr}(\text{NO}_3)_2$ ,  $\text{Ca}(\text{NO}_3)_2$ , and  $\text{CuO}$  was annealed at 850° in air for 180 hr with intermediate grindings.

To determine oxygen nonstoichiometry in the single-phase region, iodometry analysis was used. Before analysis, samples were annealed at different temperatures and  $P_{\text{O}_2}$  and quenched in air or liquid nitrogen. DTA and thermogravimetry (TGA) data were obtained using a Sartorius thermobalance (Germany) with a Pt–Pt/Rh 10% thermocouple. The heating rate did not exceed 5 K/min. Dilatometry investigations were carried out in different atmospheres with Netsch commercial equipment (Germany) at 750–950°C with a heating rate of 2 K/min. High-temperature  $ac$  resistivity measurements were made in air and in an oxygen atmosphere using Pt-electrodes ( $f = 1$  kHz). For each temperature the equilibrium between the samples and the gaseous phase was reached by isothermal exposition. In the gaseous phase, the partial pressure of oxygen ( $P_{\text{O}_2}$ ) was detected and controlled by the EMF method with the solid state electrolyte cells of  $\text{ZrO}_2$  doped with  $\text{CaO}$ . Coulometric measurements were carried out on homemade laboratory equipment with the same solid electrolyte cell. The electrical resistivity was measured as a function of temperature by a conventional  $dc$  four-probe method. Values of transport  $j_c$  were measured by an inductional technique under helium.

## 3. RESULTS AND DISCUSSION

### 3.1. High-Temperature Boundary of Phase Stability

To determine the high-temperature boundary of phase stability, we used dilatometry and TGA techniques. Peritectic melting leads to the large changes in the length of samples. The melting of samples is followed by large mass changes that are connected with oxygen losses. In simul-

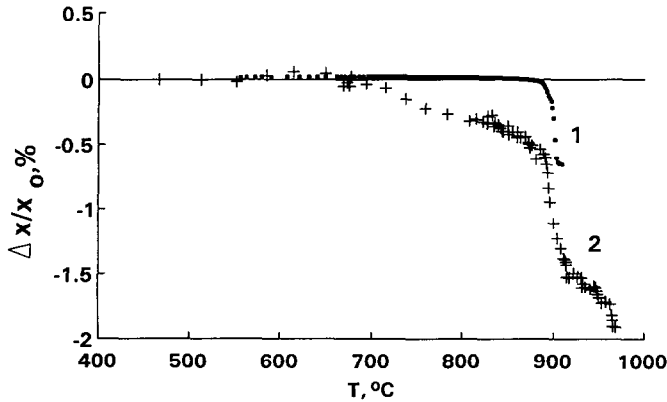


FIG. 1. Typical curves for  $\Delta l/l_0$  (1) and  $\Delta m/m_0$  (2) versus temperature (heating in air, 2 K/min) for the 2212 phase.

taneous coulometric and resistivity measurements, the sharp decrease in sample resistivity, along with the formation of a liquid phase, indicates the beginning of the strong oxygen desorption (the increase in coulometric cell current).

These methods give the opportunity to determine the melting temperatures in different gaseous atmospheres. The typical curves for  $\Delta m/m_0$  and  $\Delta l/l_0$  versus temperature are given in Fig. 1. The obtained experimental dependencies for resistivity  $R$  and coulometric cell current  $I$  versus temperature are given in Fig. 2 for  $P_{\text{O}_2} = 5.01 \times 10^{-5}$  atm. All experimental data are presented in Fig. 3 and in Tables 1 and 2.

The correlations between  $P_{\text{O}_2}$  and melting temperature  $T$  for phases 2212 and 2223 are given, respectively, by

$$-\log P_{\text{O}_2} = (-24.23 \pm 0.21) + (28.6 \pm 1.3) \cdot (10^3/T) \quad [1]$$

$$-\log P_{\text{O}_2} = (-22.59 \pm 0.29) + (26.7 \pm 1.7) \cdot (10^3/T). \quad [2]$$

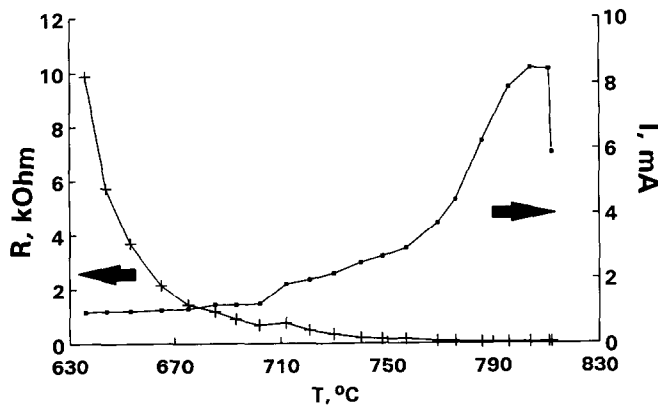


FIG. 2. Experimental curves for coulometric cell current  $I$  and sample resistivity  $R$  versus temperature (heating rate, 2 K/min,  $P_{\text{O}_2} = 5.01 \times 10^{-5}$  atm) for the 2223 phase.

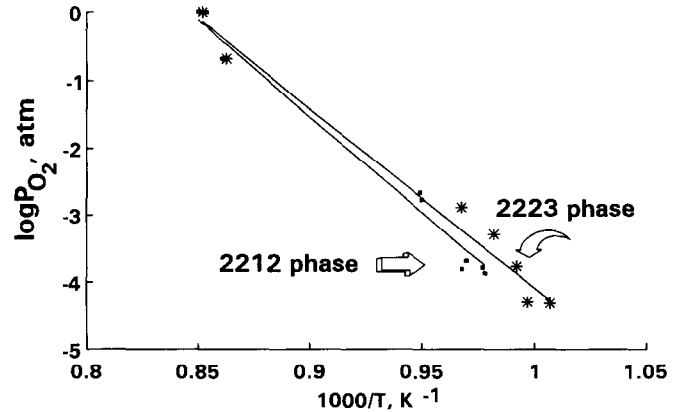


FIG. 3. High-temperature boundaries of phase stability for the 2212 and 2223 phases.

Taking into account the measurement error, the experimental data showed no differences between temperatures of melting for the 2212 and 2223 phases for the same  $P_{\text{O}_2}$ . Our experimental results are in good agreement with data of Bessergenev *et al.* (10) for air and at Rubin *et al.* (11) for low  $P_{\text{O}_2}$  values.

From the results obtained, the temperatures of synthesis and sintering in different gaseous atmospheres without liquid phase formation can be determined.

### 3.2. Low-Temperature Boundary of Phase Stability

To determine the eutectoid decomposition temperatures we used the high-temperature resistivity method. This method is very sensitive in detecting any structural or phase changes in the material. Experimental results for different  $P_{\text{O}_2}$  are described in coordinates  $\ln R = f(1/T)$ . The data obtained for sample 2212 in air are presented in Fig. 4. These curves have two linear parts. The characteristic temperatures ( $T_{\text{dec}}$ ) below which the resistivity properties of the samples changed greatly were determined from the intersection of these lines. The temperatures obtained for the 2212 and 2223 phases are presented in Table 3.

TABLE 1

The Melting Temperatures in Different Atmospheres for 2212 and 2223 Compositions Determined by Means of TGA (TG) and Dilatometry (dil)

Atmosphere	$\log P_{\text{O}_2}$ (atm)	Bi-HTSC		
		2212 Phase		2223 Phase
		$T$ (TG), °C	$T$ (dil), °C	$T$ (dil), °C
Oxygen	0	$903 \pm 5$	$898 \pm 3$	$901 \pm 3$
Air	-0.68	$886 \pm 5$	$888 \pm 3$	$886 \pm 3$

TABLE 2

The Melting Temperatures for 2212 and 2223 Compositions Determined by Means of Resistivity and Coulometric Experiments at Low  $P_{O_2}$

2212 Phase		2223 Phase	
$\log P_{O_2}$ (atm)	$T \pm 3$ (°C)	$\log P_{O_2}$ (atm)	$T \pm 3$ (°C)
-2.66	781	-2.89	760
-2.77	780	-3.29	745
-3.69	758	-3.77	735
-3.79	751	-4.30	730
-3.81	761	-4.32	720
-3.87	750		

We correlated these large changes in resistivity properties with phase changes in the samples. To prove this supposition the pellets of the 2212 phase were annealed at 840 and 770°C for 100 hr in air, and quenched. The powder X-ray data showed (Fig. 5) that the sample annealed at 770°C was not single-phase; the presence of  $Bi_2Sr_2CuO_{6+\gamma}$  and  $(Sr, Ca)Bi_2O_4$  phases (approximately 5–10 mass%) was detected. After annealing at 840°C the presence of any recorded phase was not detected by the X-ray method. Wu *et al.* (12) confirmed the formation of a  $Bi_2Sr_2CuO_{6+\gamma}$  phase, bismuth oxides, and strontium bismuth oxides after annealing single crystals of 2212 in air at 400–750°C. Similar results have been obtained for the  $Bi_{1.8}Pb_{0.4}Sr_2Ca_2Cu_3O_{10+\delta}$  phase (2). The formation of  $Bi_2Sr_2CaCu_2O_{8+\delta}$  and  $Ca_2PbO_4$ -type phases was observed after annealing in oxygen in the temperature range 790–800°C. These results confirm that the data given in Table 3 describe the low-temperature boundary of the phase stability of 2212 and 2223 compounds.

### 3.3. Oxygen Nonstoichiometry and Superconductivity Properties of $Bi_2Sr_2CaCu_2O_{8+\delta}$

The determination of the oxygen nonstoichiometry of the 2212 phase was carried out only in the regions of homogeneity. The results of chemical analysis, critical

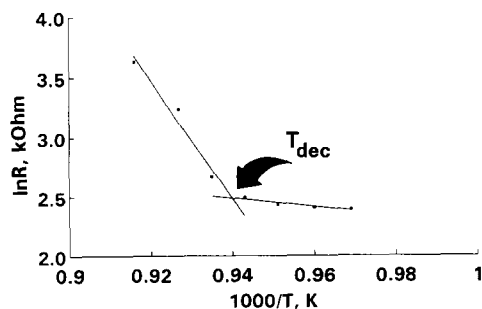


FIG. 4. Experimental dependence  $\ln R$  versus  $1/T$  and determination of decomposition temperature ( $T_{dec}$ ) for the 2212 phase in air.

TABLE 3

Phase Decomposition Temperatures for 2212 and 2223 Composition

		Bi-HTSC	
		2212 Phase	2223 Phase
Atmosphere	$\log P_{O_2}$ (atm)	$T$ (°C)	$T$ (°C)
Oxygen	0	$795 \pm 5$	$833 \pm 5$
Air	-0.68	$790 \pm 5$	$820 \pm 5$

temperatures ( $T_c$ ), and transport current density ( $j_c$ ) of the samples quenched after annealing at different temperatures and  $P_{O_2}$  are listed in Tables 4 (air) and 5 (low  $P_{O_2}$  values).

The results obtained show that in the measured range of temperatures and  $P_{O_2}$  the oxygen nonstoichiometry changes from  $\delta = 0.07$  to  $\delta = 0.22$ . The negative value  $\delta = -0.01$  from Table 5 ( $\log P_{O_2} = -3.12$  atm,  $T = 800^\circ\text{C}$ ) can be explained by too high an annealing temperature and the beginning of the melting of the sample. As can be seen from Table 4 the samples annealed in air in the temperature range 800–860°C, followed by quenching, have no differences in  $T_c$  and  $j_c$ . However, Deshimaru *et al.* (9) affirm that further increasing the oxygen content (to a value of 8.25) leads to a significant decrease in  $T_c$  (down to 80 K). In our opinion, since oxidation was carried out at 600°C in their work, the physical adsorption of additional oxygen (over a value of 8.22) took place on the surface of the samples and could be the reason for the  $T_c$  decrease. The partial phase decomposition is another

TABLE 4

Oxygen Content, Critical Temperatures ( $T_c^{on}$ , Onset;  $T_c^{end}$ , Offset, in K), and Current Density ( $j_c$ , in A/cm<sup>2</sup>) of 2212 Samples Quenched after Annealing in Air

Sample No.	$T_{ann} = 800^\circ\text{C}$				$T_{ann} = 860^\circ\text{C}$			
	$8 + \delta$	$T_c^{on}$	$T_c^{end}$	$j_c$	$8 + \delta$	$T_c^{on}$	$T_c^{end}$	$j_c$
1	8.22	91.3	69		8.16	88.5	67.9	
2		91.7	69.2					
3	8.22	109.9	77.9		8.21	102.1	78	
4	8.21				8.18			
5	8.21			1761				1529
6	8.21	89.8	66			87.1	70.4	
7	8.21				8.18			
8	8.20				8.18			
$8 + \delta$	8.212	96	71		8.187	93	72	
SD	0.007	8	4		0.018	7	4	

Note.  $8 + \delta$  is the average value of oxygen content and SD is the standard deviation.

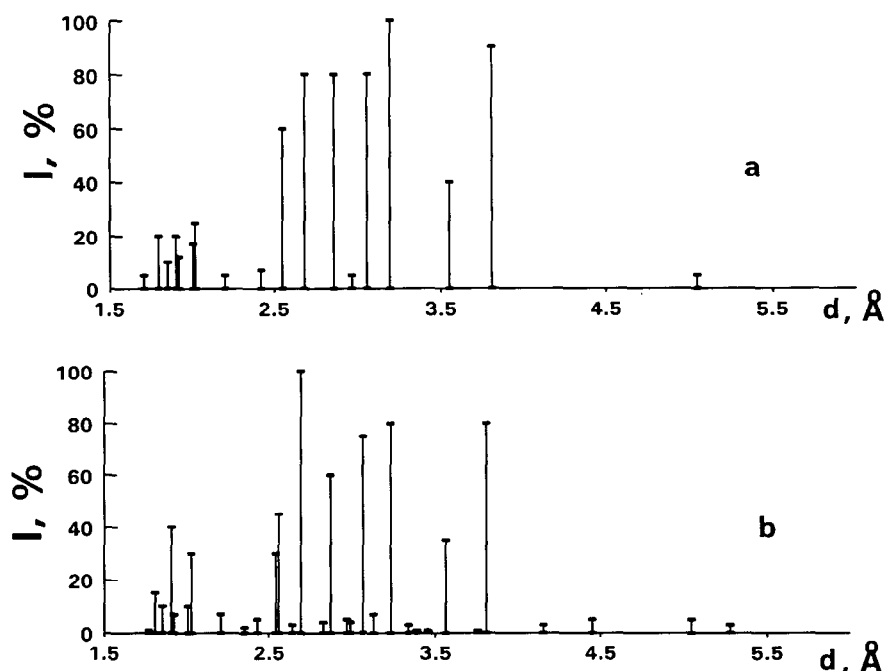


FIG. 5. X-ray data of 2212 samples annealed at 840 (a) and 770°C (b) for 100 hr.

possible reason for the decrease in  $T_c$ , because the annealing temperature during oxidation is outside of the range of phase stability.

The experimental data for slow cooled samples are presented in Table 6. The comparison of data from Tables 4 and 6 shows that after slow cooling to room temperature the samples had lower  $T_c$  and  $j_c$ , with the values of  $j_c$  strongly depending on the cooling rate. Chemical analysis of these samples ( $T_{\text{ann}} = 800^\circ\text{C}$ ) showed that oxygen content ( $8 + \delta$ ) was 8.17–8.18. Obviously, during slow cooling partial oxygen loss takes place. This is in agreement with literature data (13) concerning the existence of two types of oxygen ions in Bi-HTSC with different energy of bonding with the crystalline lattice.

Coulometric data can be interpreted from the existence of two types of oxygen ions in Bi-HTSC. The results of three experiments on the samples annealed at  $800^\circ\text{C}$  in air and quenched are given in Table 7. The  $\delta_0$  and  $\delta_k$  are initial and final values of oxygen nonstoichiometry, respectively. Negative final values  $\delta_k$  are connected with the beginning of sample melting.

TABLE 5  
Oxygen Content of 2212 Samples Quenched after Annealing at Low  $P_{\text{O}_2}$  Values

$\log P_{\text{O}_2}$ (atm)	–3.12		–3.69		
$T_{\text{ann}}$ ( $^\circ\text{C}$ )	750	780	800	700	740
$8 + \delta$	8.15	8.07	7.99	8.17	8.15

The obtained data show that a 5–10% excess over the stoichiometric oxygen amount ( $\delta_0 = 0.20$ ) can easily move away from the sample at relatively low temperatures. Probably an analogous process takes place during slow cooling in air. This can lead to the decomposition of the 2212 phase during slow cooling and additional low temperature treatment. From our point of view these processes could be the reason for the decrease in transition temperature. This is evidenced by the results of other work (2) and our experimental data. The large transition width (see Table 4) can be explained by the occurrence of these processes in spite of the quenching of samples from the annealing temperature down to room temperature. As can be seen, the rate of this quenching is not high enough.

TABLE 6  
Critical Temperatures ( $T_c^{\text{on}}$ , Onset,  $T_c^{\text{end}}$ , Offset, in K) and Current Density ( $j_c$ , in  $\text{A}/\text{cm}^2$ ) of 2212 Samples after Annealing (5 hr, in Air) Followed by Slow Cooling

$T_{\text{ann}}$ ( $^\circ\text{C}$ )	$T_c^{\text{on}}$	$T_c^{\text{end}}$	$j_c$
800	77.0	62.5	1110 <sup>a</sup> 172 <sup>b</sup>
830	76.7	63.8	
860	76.1	64.0	
$T_c^{\text{ave}}$	76.6	63.4	
SD	0.4	0.7	

Note.  $T_c^{\text{ave}}$  is the average value of  $T_c$ , SD is the standard deviation.

<sup>a</sup> Cooling rate is 4 K/min.

<sup>b</sup> Cooling rate is 0.4 K/min.

TABLE 7

Oxygen Content Changing ( $\delta_0$  and  $\delta_k$  Are the Initial and Final Values of Oxygen Nonstoichiometry, Respectively) of 2212 Samples during Heating under Nitrogen ( $P_{O_2} = 10^{-4.2}$  atm)

Sample No.	$\delta_0$	$T$ (°C)	$\delta_k$
1	0.20	445–700	0.15
		800–850	–0.06
2	0.20	400–450	0.19
		750–800	0.01
3	0.20	400–450	0.19
		780–820	–0.03

Consequently, to obtain high critical parameters of the 2212 and 2223 ceramics, it is necessary to quench the samples after high-temperature treatment in liquid nitrogen. In addition, it is necessary to consider the influence of cation nonstoichiometry, for example the Sr/Ca ratio (7, 9), in order to avoid a possible ambiguity in the explanation of any change in superconductivity properties. These experiments are in progress now.

#### 4. CONCLUSION

Phase stability of  $\text{Bi}_2\text{Sr}_2\text{CaCu}_2\text{O}_{8+\delta}$  and  $\text{Bi}_{1.8}\text{Pb}_{0.4}\text{Sr}_2\text{Ca}_2\text{Cu}_3\text{O}_{10+\delta}$  was studied by TGA, dilatometry, high-temperature resistivity, and X-ray methods in the 700–1000°C temperature range and  $P_{O_2} = 1-10^{-4.3}$  atm. The existence of a high-temperature boundary of phase stability (peritectic melting) was found. The phenomenon of low-temperature phase decomposition was detected in air and under an oxygen atmosphere.

The change in oxygen content was determined for the  $\text{Bi}_2\text{Sr}_2\text{CaCu}_2\text{O}_{8+\delta}$  phase in the 700–860°C temperature range,  $P_{O_2} = 0.21-10^{-3.7}$  atm by iodometric analysis of the quenched samples. It was determined that in the single-phase region the change in oxygen nonstoichiometry has an insignificant influence on  $T_c$ . The slowly cooled samples have lower values of  $T_c$  and  $j_c$  in comparison with the quenched ones. We suppose that during slow cooling and additional low-temperature treatment two processes take place: phase decomposition and a decrease in oxygen content. These processes lead to lessening of superconductivity properties. The fast quenching of  $\text{Bi}_2\text{Sr}_2\text{CaCu}_2\text{O}_{8+\delta}$  and  $\text{Bi}_{1.8}\text{Pb}_{0.4}\text{Sr}_2\text{Ca}_2\text{Cu}_3\text{O}_{10+\delta}$  samples after high-temperature treatment was suggested.

#### REFERENCES

1. Y. Idemoto and K. Fueki, *Physica C* **168**, 1 and 167 (1990).
2. I. F. Konotyuk, V. V. Vashuk, L. V. Makhnach, and Yu. G. Zonov, *Supercond. Phys. Chem. Technol.* **3**, 282 (1990).
3. N. Miura *et al.*, *Jpn. J. Appl. Phys.* **28**, L1112 (1989).
4. J. Bock, E. Preisler, and S. Elschner, in "ICMAS de la SUPRA-CONDUCTIVITE d'aujourd'hui aux Applications" p. 539. Frankreich, Grenoble, 1990.
5. T. Ishida and T. Sakuma, *Jpn. J. Appl. Phys.* **27**, L1237 (1988).
6. Bochimi *et al.*, *Physica C* **159**, 654 (1989).
7. P. Majewski, H. L. Su, and B. Hettich, *Adv. Mater.* **4**, 508 (1992).
8. T. G. Holesinger *et al.*, *Physica C* **202**, 109 (1992).
9. Yu. Deshimaru *et al.*, *Jpn. J. Appl. Phys.* **30**, L1798 (1991).
10. V. G. Bessergenev, A. A. Kamarzin, H. Bach, and M. O. Klimenkov, *Supercond. Sci. Technol.* **5**, 440 (1992).
11. L. M. Rubin *et al.*, *Appl. Phys. Lett.* **61**, 1977 (1992).
12. W. Wu, *et al.*, *J. Appl. Phys.* **74**, 7388 (1993).
13. J. T. S. Irvine and C. J. Nangung, *Solid State Chem.* **87**, 29 (1990).